Biosensors and Bioelectronics 126 (2019) 697–706

Contents lists available at ScienceDirect

Biosensors and Bioelectronics

journal homepage: www.elsevier.com/locate/bios

Microfluidic chip coupled with optical biosensors for simultaneous detection of multiple analytes: A review

Zerong Liao[a,1], Yang Zhang[b,1], Yongrui Li[a,1], Yunfei Miao[a], Shimeng Gao[c], Fankai Lin[a], Yulin Deng[a], Lina Geng[a,*]

[a] School of Life Science, Beijing Institute of Technology, 5 South Zhongguancun Street, Haidian District, Beijing 100081, PR China
[b] College of Science, Harbin Institute of Technology (Shenzhen), Shenzhen, China
[c] College of Agriculture and Life Sciences, University of Wisconsin-Madison, Madison, WI 53706, USA

ARTICLE INFO

Keywords:
Microfluidic chip
Optical sensor
Multiplex detection

ABSTRACT

This article reviews the recent advances in microfluidic-chip integrated optical biosensors for simultaneous detection of multiple analytes. In particular, the principles and recent progress in different kinds of multiplex optical biosensors and their biological application were reviewed comprehensively. Sensors based on multiplexed detection have absolute advantages in analysis throughput than single assay. The microfluidic chip, a type of micro-total analysis system (μTAS), provides an ideal platform for integration of high-throughput biosensors. Compared with electronic biosensors, benefitted from the technical development in Micro-Electro-Mechanical System, there have been greater advances in the fabrication of optical sensors and microfluidic chip, and then promoting microfluidic-chip integrated optical biosensors for simultaneous detection of multiple analytes.

1. Introduction

As the result of the complexity, biomedical diagnostic based on single-analyte assays can only provide limited information. Multiplex biosensors have many advantages over single-analyte assays, which increase the test throughput and improve test efficiency. The fabrication of suitable multiplex devices is of utmost importance for the development of quick, high-throughput, compact miniaturized and low-cost solutions for biomedical diagnosis. Therefore, it has been great enthusiasm in recent years for developing multitarget analysis using parallel single-analyte or simultaneous multianalyte detection, especially in optical biosensor (Bakaltcheva et al., 1999; Faulds et al., 2010; Nyholm, 2005; Srinivasan et al., 2003).

Being one of the most commonly reported biosensors, an optical biosensor combines a biorecognition sensing element with an optical signals detection system, measuring changes in light when binding analytes (Douglass et al., 2002). Various optical techniques have been adapted into biosensors include optical fibres, fluorescence, luminescence, wave guides, surface plasmon resonance and microarrays (Ferguson et al., 1996; Guan et al., 2010; Ince and Narayanaswamy, 2006; Wang et al., 2010). Optical biosensors shows enormous advantages such as less interference, high sensitivity and specificity, low background noise signal, etc. (Cooper, 2006). Most importantly, the possibility of multiplexing by measuring different wavelengths signals from multiple analytes offers powerful new analytical tools (Emmerson et al., 2010).

Benefited from the small sample volumes, ease of multiplexing and integration, rapid turnaround times and high portability offered by microfluidics, microfluidic chip are one of the most striking technologies which have been integrated with increasing numbers of optical biosensor systems to improve the overall performance of the detection systems (Arduini et al., 2017).

There are some scientific literature with reviews of singular, specific topics related to sensors, microfluidic-based sensors and simultaneous multisensoring (Bunyakul and Baeumner, 2014; Ferrier et al., 2015; Ge et al., 2014; Holzinger et al., 2014; Jadon et al., 2016; Jiang et al., 2014; Kelley et al., 2014; Muzyka, 2014; Rocha-Santos, 2014; Sang et al., 2014; Van et al., 2014). However, there has been no report on microfluidic chip integrated optical biosensors for multiplexed detection until now. Due to the burgeoning development of micro-optics, there are gradually more advances for optical biosensors than for electronic sensors. The new published literatures in 2018 focused on optical sensors reflected its role of hotspots in multicomplex sensors. In this paper we tried to provide a comprehensive overview including the

* Corresponding author.
E-mail address: gln@bit.edu.cn (L. Geng).
[1] Those authors contributed equally to this work.

https://doi.org/10.1016/j.bios.2018.11.032
Received 29 August 2018; Received in revised form 13 November 2018; Accepted 19 November 2018
Available online 20 November 2018
0956-5663/

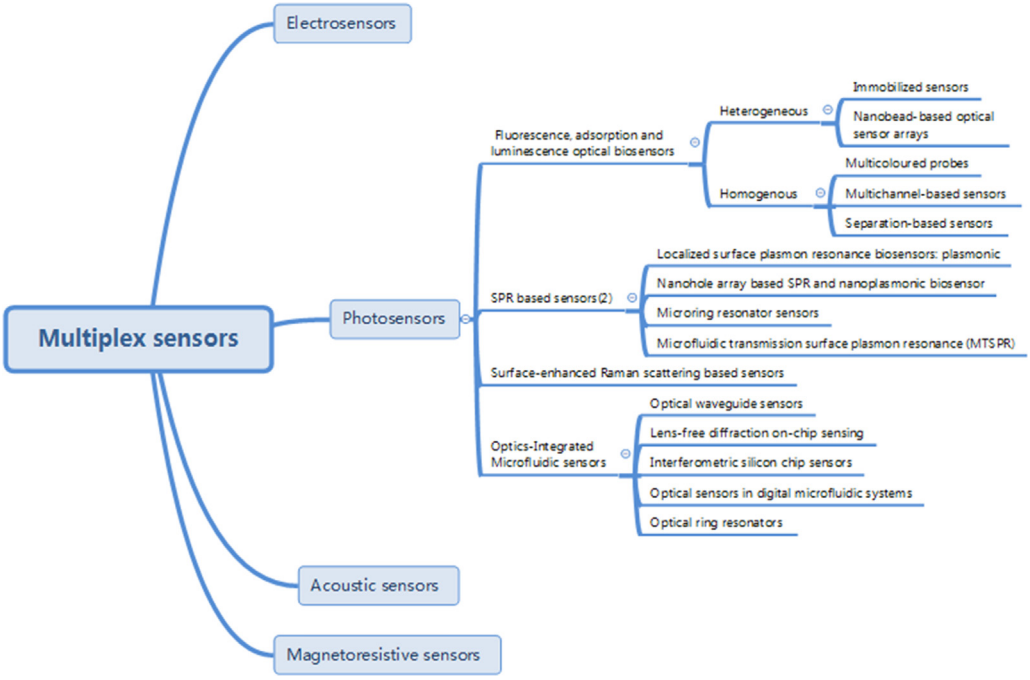

Fig. 1. A taxonomic diagram of optical sensors integrated with microfluidic chips for multiplexed assays.

principles and recent development in different kinds of multiplex optical biosensors integrated with microfluidic chip for biological application mainly from 2010 onwards.

2. Multiplex optical sensors combined with microfluidics

Optical biosensors can analyse chemical and biological reactions by measuring light absorption, reflectance, fluorescence, and luminescence. Multiplex Optical Sensors can also be categorized in the same way as traditional optical biosensors for single analyte. In order to give a clear picture about the review contents, a taxonomic diagram (Fig. 1) with the summary of the recent development of microfluidics-based multiplexed optical biosensors is presented, including fluorescence optical sensors and traditional optics based sensors.

2.1. Fluorescence and luminescence biosensors

Fluorescence- and luminescence-based biosensors are the prevalent types of optical biosensors coupled with microfluidic chips, with advantages such as ease of implementation, low detection limits, high selectivity and lots of chemical fluorescence labels available (Lafleur et al., 2016). These sensors can be divided into heterogeneous mode and homogenous mode, depending on whether the sensors are immobilized on the chip substrate or not. Immobilized sensors, nanobead-based sensor arrays and dedicated optical fixtures such as lenses and microspectrometers are classified as a large family of heterogeneous mode. Meanwhile, fluorescent optical sensors floating in solution typically represent the other class, homogenous mode.

2.1.1. Heterogeneous fluorescence and luminescence biosensors

Optical sensor arrays on chips were developed using monolayers with metal-ion-sensing properties self-assembled on the inner walls of five parallel microchannels (Basabedesmonts et al., 2008). A supramolecular luminescent sensor platform with five parallel sensing self-assembled monolayers (SAMs) was also implemented in a microfluidic device. A Eu(III)-EDTA complex was self-assembled through a host-guest interaction with β-cyclodextrin monolayers. A highly luminescent lanthanide complex was further formed by the Eu(III)-EDTA and naphthalene β-diketone, which acted as an antenna. Multiplexed phosphate and carboxylic acid screening was demonstrated with micromolar and nanomolar detection sensitivity, respectively (Bilge et al., 2011). Multivalent aptasensor array was built up in the channel of microfluidic devices for the detection of two biomarkers. The fluorescence was amplified with silver aggregated (Z.H. Liu et al., 2018; X.H. Liu et al., 2018).

Recently, a Förster resonance energy transfer (FRET)-based 'signal-on' aptasensing strategy, with its efficiency, selectivity and sensitivity, has attracted increasing attention. In fluorescence biosensors, when the fluorescent emission spectrum of the donor molecule overlaps with the absorption spectrum of the receptor molecule and the distance between the two molecules is 10 nm or less, FRET occurs due to non-radioactive energy transfer through long-range dipole-dipole interactions (Surade et al., 2010). One chip aptasensor was prepared by binding DNA and RNA aptamers to a graphene oxide (GO) surface. Multiple-target detection of thrombin and prostate was demonstrated with a 2 × 3 linear-array GO aptasensor (Ueno et al., 2015). Qi reported a three-dimensional (3D) origami ion-imprinted polymer (IIP) microfluidic paper-based chip device, made by grafting CdTe QDs, for specific, sensitive and multiplexed detection of Cu^{2+} and Hg^{2+} ions. The occupancy of IIP/CdTe QD complexes by Cu^{2+} or Hg^{2+} led to fluorescence quenching of QDs because of the photoluminescent energy transfer. Compared with a floating QD quenching sensor system, the immobilized QD quenching platform allows simultaneous detection with improved selectivity and sensitivity (Qi et al., 2017).

The emergence of porous-bead-based high-density planar microarrays with high surface-to-volume ratio, encoding capabilities, modest sample volume requirements and highly parallelized production presents a novel, easy method for parallelized, high-throughput testing and validation (Chou et al., 2012). A modular microfluidic biosensor integrated with QDs for the multiple quantitation of three cancer markers CEA, CA125, and Her-2/Neu (C-erbB-2) was achieved. In this sandwich-type immunoassay, QD-labelled detecting antibody binds to the antigen and is captured by a microporous agarose bead array within the chip. The performance of the system, with integrated sample pretreatment, target capture and final detection modalities, was demonstrated with real specimens of serum and saliva (Jokerst et al., 2009).

An ideal detection particle for a porous-bead-based microchip sensor should have high information content for multiplexed detection

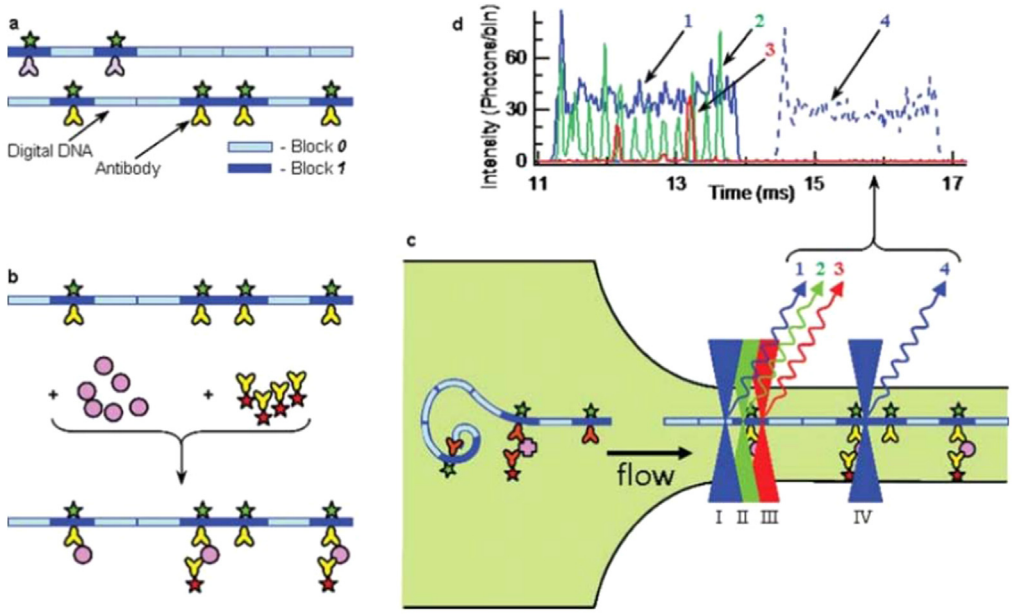

Fig. 2. Schematic of a suspension array based on digital DNA. (a) Digital DNA molecules built of two blocks, 1 and 0, generating many distinct bar codes. (b) Analytes (circles) binding to the DNA-bound antibodies also serve as bridges for the red-labelled secondary antibodies (red stars). (c) Stretched DNA molecules are interrogated with light beams I–IV in the microfluidic device. (d) Representative signals of digital DNA (Burton et al., 2010). Reproduced by permission of the Royal Society of Chemistry.

and miniaturization, and can be fabricated in an easy way and at low cost. Being a solid-state molecular wire, DNA can be easily manipulated to carry a wealth of information, which makes it an attractive alternative to the polystyrene beads commonly used in existing suspension arrays. High multiplexing with high sensitivity was then realized with a suspension array sensor built from specially designed recombinant digital DNA that carried both specific analyte recognition units and encoded units (Fig. 2) (Burton et al., 2010). Subsequently, a DNA microsphere-based immunoassay was integrated into a microfluidic device, yielding an LOC approach that could screen an antigen–antibody pair in the same sample by the logic operations AND and INHIBIT. With the clinically relevant biomarkers TNF-α (a cytokine) and anti-TNF-α antibody as a model, an output of AND indicated the presence of both inputs, while a different fluorescent signal output of INHIBIT indicated the presence of only one specific input (Sabhachandani et al., 2015).

One kind of online analysis setup based on core–shell nanosensors was fabricated for simultaneous detection. Two different lipophilic indicator dyes, platinum (II) meso-tetra(4-fluorophenyl)tetrabenzoporphyrin (PtTPTBPF) and BF2-chelated tetraarylazadipyrromethene dye (aza-BODIPY), were incorporated respectively into poly(styrene-*block*-vinylpyrrolidone) nanoparticles with a core–shell structure to produce nanosensors for oxygen and pH. Such nanosensors have several advantages including excitability with red light, emission wavelengths in the near-infrared spectral region, high stability, and the capacity for contactless read-out with adapted oxygen metres (Ehgartner et al., 2016). Photonic crystal encoded microbead-based arrays are a new type of modular sensor ensemble technology. Solvent-responsive photonic encoded microbeads with reflection peak position at 487 nm, 565 nm and 725 nm were integrated with microfluidic chips to realize low- to medium-throughput multiplex immunoassays. In addition to amplifying the fluorescent intensity, RBMs (responsive breathing microbeads) with restored encoding signal could also be used for multiplex detection (Luan et al., 2017). Moreover, RBMs could bring better repeatability and higher sensitivity than silica colloidal crystal beads (SCCBs) (Luan et al., 2017). NPs have become powerful candidates for array-based sensing platforms. Essential issues regarding the scalability of these sensor arrays were explored in a review (Bigdeli et al., 2017). The main characteristics and processes of most common NP-based optical sensor arrays were also described in a recent review. The principles of optical sensor arrays, different types of plasmonic and fluorescent NPs, the fundamental steps in the design of a sensor array together with the details of each step, the main criterion of cross-reactivity, chemometric data analysis, and the vast number of applications of NP-based optical sensor arrays were discussed (Bigdeli et al., 2017).

2.1.2. *Homogenous fluorescence and luminescence biosensors*

Compared with heterogeneous assay sensors, homogenous optical sensors can improve simplicity and robustness, facilitate automation, and allow upgrading for multiple assays (Heyduk et al., 2008; Wang et al., 2011). Currently, electrochemical sensors are all carried out only in a heterogeneous manner; therefore, and then homogeneous sensing is a unique feature of optical sensors. In the same way as heterogeneous assay to simultaneous parallel sensing of multiple targets, in a homogenous assay with suspended sensors, multicoloured probes were also used to discriminate signals from different sensors. However, the number of coloured probes available is limited, to say nothing of the challenge existed in reading out and discriminating multi-coloured signal in floated mixture without spatial separation in a single micro- or nanochannel. In order to address this difficulty, the strategy of multi-channel-based multiplex sensors was employed. Although sequential assays of sucrose, D-glucose and D-fructose via cascade of specific enzymatic reactions could be carried out in a model optimized microfluidic chip with an integrated optical detection system. While parallel implementation of the assays was necessary in order to further improve the throughput (Atalay et al., 2009). Le and Kim published a rapid and portable method using quantum dot-based FRET for simultaneous detection of the mutant alleles of codons 12 and 61 of the NRAS gene (NRAS Proto-Oncogene) in a multichannel microfluidic chip. Bead/QD/DNA probe assemblies and dyes intercalated inside the double-stranded DNA were used to detect the target DNA. DNA hybridization resulted in fluorescence quenching of the QDs due to FRET between QDs and dyes (Le and Kim, 2014). A multiplex cancer cell sensor chip was also created by an aptamer/GO-based FRET strategy. Seven different cancer cell samples could be measured at the same time by parallel homogenous detection (Cao et al., 2012). A simple microfluidic biosensor including QD–enzyme conjugates entrapped in a hydrogel microstructure in a set of microchannels was fabricated for multidetection. H_2O_2 was produced from catalytic oxidation of glucose and alcohol by enzymes conjugated to QDs and quenched the fluorescence of the QDs. The intensity of fluorescence decreased with increasing concentrations of glucose and alcohol. The LODs for glucose and alcohol were 50 μM and 70 μM, respectively (Jang et al., 2012). In recent literature using

Mn:ZCS@ZnS nanorods with a high fluorescence quantum yield, the limit of detection for glucose can reach to 100 nM. If these new techniques as such were introduced into multicomplex sensors, the LODs of simultaneous sensoring will also be greatly improved (Shen et al., 2018).

Without the need to fabricate multiple channels for the sake of portability, and making use of the flow characteristic, another kind of electrophoresis separation-based FRET multisensor with a single label in a single microfluidic channel were developed. Two basic steps were involved. The first was classic aptamer/GO-based FRET. After the addition of the sample mixture, the binding of the target proteins with their corresponding aptamers led to the detachment of oligonucleotides from GO, which brought about selective recovery of the fluorescence of carboxyfluorescein (FAM)-labelled aptamers. Microfluidic chip electrophoresis provided multiplex discrimination through the enrichment and separation of every protein-aptamer binding pair in the mixture. With no need for multicoloured probes, sensor immobilization or sample pretreatment, this technique of separation-based optical sensors provides an extremely easy and convenient method for simultaneous and high-throughput optical multianalyte sensing with fine spatial resolution. The target analytes themselves need not be detected by UV or fluorescence. At the same time, high sensitivity is guaranteed by the high separation ability of chip capillary electrophoresis (CE), the electrophoresis-induced enrichment, and the low background noise due to the super-quenching ability of GO and the selective restoration of fluorescence. Furthermore, as the separation capacity of chip-CE develops, the number of targets that can be simultaneously detected grows as well (Lin et al., 2014). This novel simultaneous sensor strategy based on separation and concentration was also developed into a simple, quick, and sensitive tool for simultaneous multi-drug screening (Lu et al., 2017) (Fig. 3).

Another integrated pH sensor using micro-free-flow electrophoresis was also reported. The study presented a microfluidic platform including an on-chip biomolecule labelling chamber followed by a continuous free-flow electrophoresis separation bed and a near-infrared fluorescent hydrogel pH sensor layer. Isoelectric focusing (IEF) of model proteins, peptides and a tryptic digest of physalaemin was carried out with this assembly (Herzog et al., 2014, 2016).

2.2. Surface plasmon resonance (SPR)-based sensors

SPR, the most widely used method for non-labelled optical biosensors, consists of the resonant oscillation simulated by incident light at the interface of two media (Fan et al., 2008). Owing to their merits of low cost and ease of integration, SPR and localized surface plasmon resonance (LSPR) have been introduced into microfluidic devices for bio-detection (Singh, 2016). However, the complex prism-coupling instrumentation in conventional SPR hampers multiplexed analysis and integration into LOC systems (Špačková et al., 2016). Nanoplasmonic biosensors characterizing nanostructures (e.g., nanoparticles, nanoapertures) can overcome the above problems and have attracted significant attention (Estevez et al., 2014). Recent advances in fabrication with electron-beam and ion-beam lithography and characterization with scanning electron and atomic force microscopy have catalysed the development of plasmonic nanostructures and the discovery of novel plasmonic phenomena. Optical biosensors based on plasmonic phenomena have given rise to extensive research (Biswas et al., 2012; Long and Jing, 2014; Špačková et al., 2016; Z. H. Liu et al. 2018; X. H. Liu et al., 2018). In addition to nanoplasmonics, other new plasmon resonance techniques, such as SPR imaging, sensors based on polarization and interferometery, etc., have also been used to construct multicomplex microfluidic chip SPR sensors.

2.2.1. Surface plasmon resonance imaging (SPRI)

In contrast to SPR with a fixed angle or wavelength, in which the reflected light is captured by a single-element detector, the reflected light in SPRI is captured by a charge-coupled device (CCD) across the sample surface. SPRI is suitable for in situ, real-time simultaneous monitoring of molecular interaction, as well as high-throughput studies (Steiner, 2004). In one microfluidic SPRI measurement, several targets can simultaneously hybridize to distinct aptamer detector elements with different capture sequences in a multiplexed aptamer microarray on the chip (Chen et al., 2012). In another report on the fabrication of microfluidic-based biosensor flow cells for SPRI multiarray immunoassays, polydimethylsiloxane (PDMS) was irreversibly adhered to plastic substrate by using a plasma-enhanced chemical-vapour-deposited SiO_2 film as the intermediate layer (Liu et al., 2011).

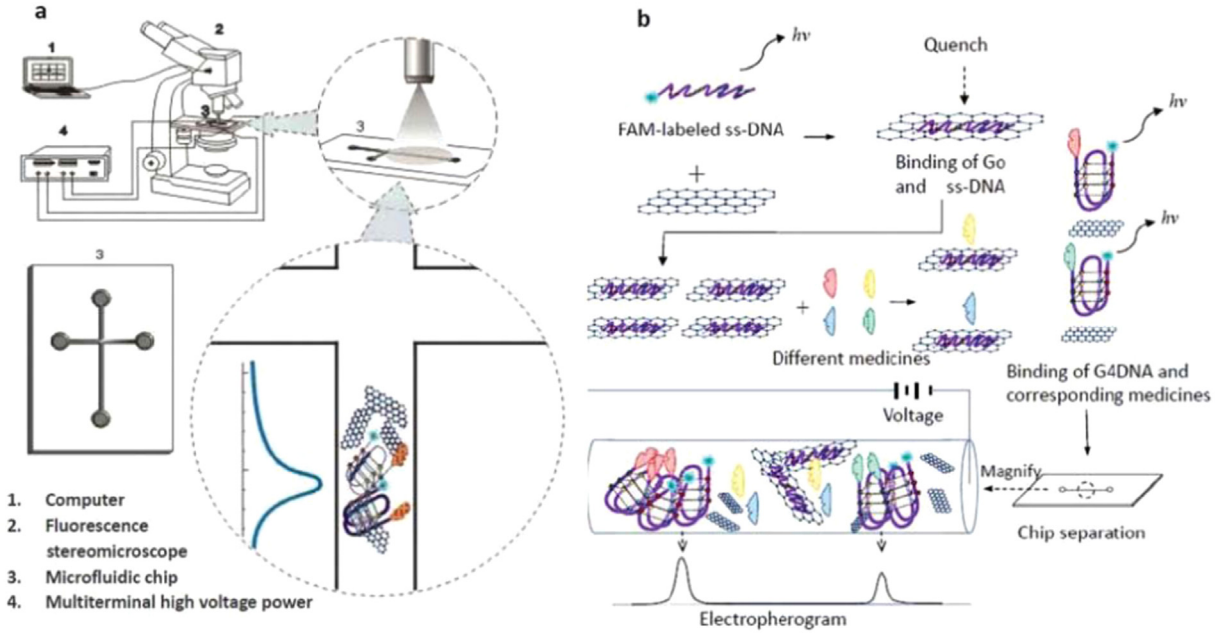

Fig. 3. (a) A schematic of the whole device; (b) a schematic diagram of an aptamer/GO-based FRET and chip-CE combination biosensor for multiple drug screening (Lu et al., 2017). Reproduced with permission of the Royal Society of Chemistry.

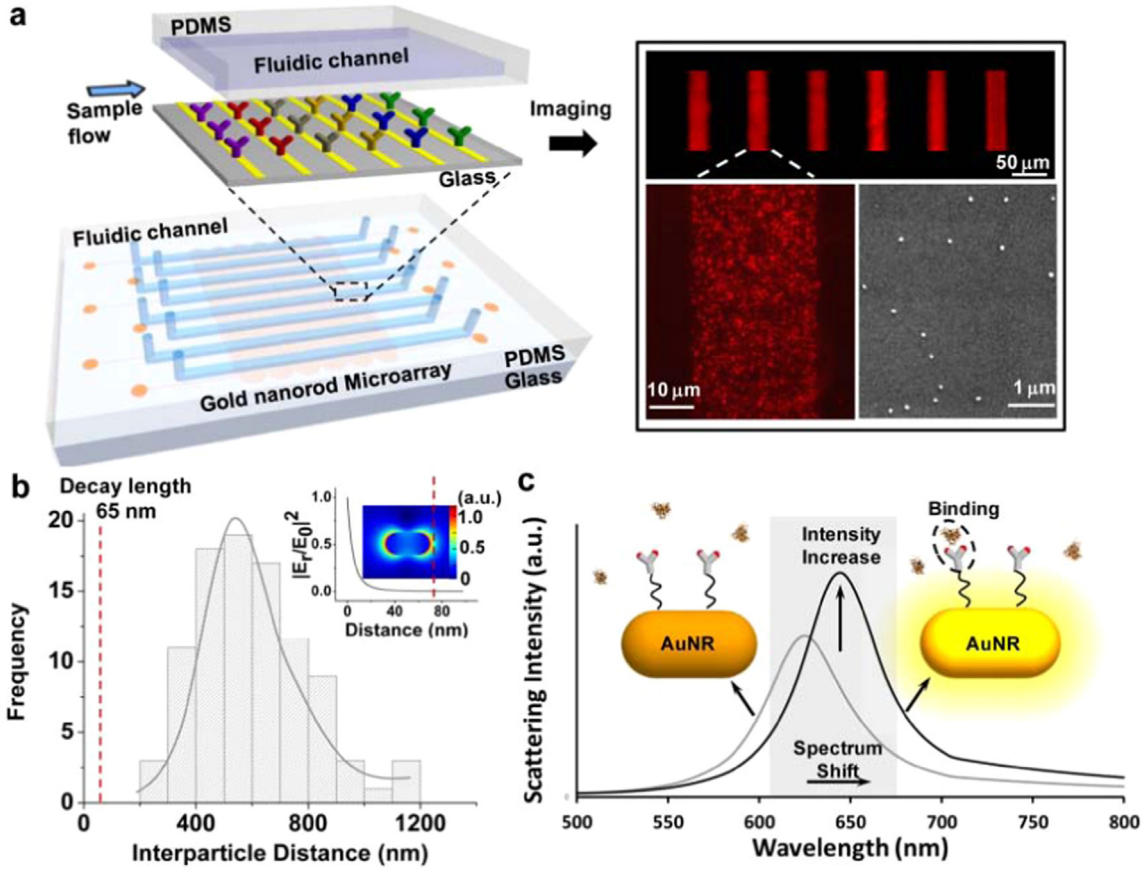

Fig. 4. (a) Schematic of a nanorod-based LSPR microarray integrated into a microfluidic chip with eight parallel channels. The prepared LSPR microarray chip was then imaged under dark-field microscopy and scanning electron microscopy (SEM). (b) Histograms of the particle-to-particle distance of the AuNRs on the LSPR microarray chip characterized using SEM images. (c) The principle of the LSPR microarray method. Analyte molecules are introduced to an antibody-functionalized AuNR LSPR biosensor. Binding of the analyte molecules to the receptors induces a redshift and scattering intensity change of the longitudinal SPR (exaggerated in the illustration). This intensity change is imaged via the characteristic frequency (gray area) using EMCCD coupled dark-field microscopy. High-sensitivity quantitative cytokine measurements at concentrations down to 5–20 pg/mL from a 1 μL serum sample was allowed by this technology. Reprinted (adapted) with permission from Chen et al. (2015). Copyright 2015, American Chemical Society.

2.2.2. LSPR biosensors

Driven by modern advances in nanofabrication, the phenomenon of LSPR is generated by a light beam trapped within metallic nanoparticles (NPs) or nanostructures whose size is smaller than the wavelength of the light (Mayer and Hafner, 2011). In LSPR, the binding of analyte molecules onto the surface is detected in real time according to a peak shift in the LSPR spectra (Anker et al., 2008; Mayer and Hafner, 2011). Compared to SPR sensors, LSPR sensors have the advantages of high-throughput sensor array capability, reduced cost of fabrication, and outstanding sensitivity (Cao et al., 2014).

For the multidetection of analytes in low concentrations, a substrate of ordered Ag nanodot arrays was used to enhance the electromagnetic field near the chip surface due to the LSPR of the Ag nanodots and thus increase the sensitivity in a microfluidic surface-enhanced Raman scattering (SERS) chip. Via a self-built inverted SERS microspectrometer, the multiplexed SERS signals of adenine and thiram were detected with an LOD of 5.0×10^{-7} M (Chen et al., 2014). Another example is a high-throughput optical biosensor device with 480 nanoplasmonic sensors in microfluidic channel arrays (Fig. 4). Parallel immunoassays of six cytokines at lower concentration in serum, down to the pg/mL scale, were demonstrated in a device fabricated using microfluidic patterning and gold nanorods (AuNRs) conjugated with antibodies. The scattering light intensity across the ensemble of AuNR microarrays was scanned with dark-field imaging optics. Complete parallel assays of a serum sample, involving sample loading, incubation, washing, and multidetection, were completed within 40 min (Chen et al., 2015). A low-cost stand-alone LSPR imaging multiparametric biosensor was developed based on a nanohole array biochip integrated with a microfluidic layer and a processing system in this compact device. A light beam from an IR light-emitting diode (LED) was focused by optics. The light reflected from the surface of the biochip was captured by a digital image sensor (Rampazzi et al., 2016). Recently an on-chip LSPR sensor was present. By versatile programming, it could perform automatic, quantitative, and multiplexed screening of biomarkers in human serum (Yavas et al., 2018).

2.2.3. Nanohole array techniques

Similar to SPR, in nanohole array (NHA) techniques, the changes of local refractive index at the sensor surface due to binding events, are detected by tracking the transmission spectra optically. The light confinement on the nanoscale allows NHAs to achieve high sensitivity. Furthermore, in the same way as LSPR, NHAs also have an outstanding ability for high-throughput multiplexing analysis and for integration into LOC devices because NHAs can be organized in a highly compact manner (Chang et al., 2011). Gold NHA-based nanoplasmonic biosensors demonstrating a capacity for label-free and multiplexed detection, which makes them a promising prospect for miniaturization (Cetin et al., 2014; Escobedo, 2013). A phenomenon of extraordinary optical transmission (EOT) was supported by sub-wavelength NHAs fabricated on optically thick metal films. EOT is created due to the strongly enhanced field near the nanoholes resulting from the excitation of plasmons by grating coupling of light at normal incidence (Ebbesen et al.,

1998). Moreover, as the EOT phenomenon avoids the prism-coupling mechanism (Nguyen et al., 2015), it is easy for the NHA-based sensor to fit into a lens-free on-chip imaging setup, ideal for miniaturization (Coskun et al., 2014; Li et al., 2017). A gold nanohole array supporting an EOT nanoplasmonic biosensor was developed, enabling label-free, sensitive, high-throughput and real-time monitoring of live-cell cytokine secretion. An adjustable microfluidic cell module was integrated for keeping cells alive and well under controlled culture conditions for 10 h which is hindered by current fluorescent and colorimetric approaches due to their dye labelling step and discrete 'snapshot' readouts (Li et al., 2017). The potential applications of NHA-based sensors to multiplexed protein binding assays, as well as the impact of applications on the instrument and assay design of NHA-based sensors, were also reviewed by Cuiffi et al. (2010). In addition, the latest advances in nanoplasmonic sensors for biointerfacial science were recently reviewed by Jackman et al. (2017).

2.2.4. Microring resonator (MRR) sensors

Label-free MRR sensors, which detect changes in bulk refractive index, can also detect a specific biological or chemical analyte after surface treatment and have attracted a great deal of attention in the field of high-throughput sensing because of their small size and sensitivity (Kwon and Steier, 2008). For a multiplexed silicon nanophotonic microring resonator lab-on-a chip biosensor, a sensor was designed and optimized systematically according to noise characteristics. The critically coupled resonators achieved the same detection limit as the conventional designs while consuming 40% less power. This optimization method can be generalized to other type of optical resonators. A CMOS-compatible process was used to fabricate the device. A swabbing lift-off technique for the deposition of the protective oxide layer increased the lift-off quality and yield. The surface of the microfluidic flow cell was functionalized with glycan receptors. Simultaneous detection of *Aleuria aurantia* lectin (AAL) and *Sambucus nigra* lectin (SNA) was tested with this sensor system (Ghasemi et al., 2016). Grimaldi presented a mirroring-resonator-based sensing platform with a polymeric microfluidic transport approach. Precise analyte dispensing and efficient transfer to the ring surface were enabled by a hole in the centre of the ring. The proposed device architecture has several advantages including simplicity, response time, selectivity and multiplexing of assays (Grimaldi et al., 2015). Without the use of a fluidic component to continuously deliver the sample to the sensor surface as in common silicon nanophotonic microring resonator sensors, digital microfluidics were integrated to increase the portability of the system. Their performance was demonstrated by performing proof-of-principle concentration measurements of glucose, sodium chloride, and ethanol (Lerma et al., 2012).

2.2.5. Microfluidic transmission surface plasmon resonance (MTSPR)

One kind of MTSPR-based biosensor was constructed by assembling a gold-coated grating substrate onto microchannels. A strong, narrow SPR peak between 650 and 800 nm was shown in the transmission SPR spectrum. This sensor chip was applied for glucose detection. The functionalization of gold-coated grating substrates facilitated the coupling/decoupling of the surface plasmon to prepare a uniform surface for sensing. The detection limit of the system for glucose was 2.31 mM. This platform opens the possibility of further development of multiplex systems, as well as practical point-of-care biosensor applications (Lertvachirapaiboon et al., 2017).

2.3. SERS-based sensors

SERS is a spectroscopic technique that combines laser spectroscopy with the special optical properties of noble metal (Au, Ag, and Cu) nanostructures with attached molecules, producing strongly increased Raman signals (Kneipp et al., 2002). Thus, the SERS-active noble metal nanostructures externally injected with the sample or built into the microchannels, as well as the specific topographical design of the channels, influence the performance of the microfluidic sensor in different ways (Zhou and Kim, 2016). Choi et al. developed a microfluidic SERS device with a programmable AgNP-based gradient for simultaneous detection. The SERS signals of the target DNA were present only on the spots with immobilized complementary DNA. The design of microfluidic channel network allowed mixtures to be injected in different concentrations. Thus, the SERS signals of two DNA sequences could be dynamically measured and quantitatively distinguished within 10 min (Choi et al., 2012). Recently, in a round microfluidic device with a rough Au surface fabricated on the electrode, electrophoresis, DEP, and electrohydrodynamic manipulations could simultaneously contribute to the concentration, separation, and in situ SERS detection of three bacterial species (*S. aureus*, *E. coli*, and *P. aeruginosa*) in blood (Cheng et al., 2013). SERS combined with microfluidic chips has been applied for sensitive optofluidic detection for more than a decade. The development of SERS combined with microfluidic chips for sensitive optofluidic detection and SERS-enabled LOC systems was summarized in a review (Huang et al., 2015; Zhou and Kim, 2016).

2.4. Optics-integrated microfluidic sensors

Traditional optical systems used in biomicrofluidics rely heavily on optical components, such as lenses, waveguides, and lasers, in the form of off-chip microscopy, which are typically bulky. The need for low-cost, sensitive and portable optically microengineered spectroscopic detection systems has yet to be met. The microelectronics industry provides efficient means to fabricate microdevices over a silicon wafer. These advanced techniques can be used equally well to create optical circuits that can be integrated into a chip (Carlborg et al., 2010). On-chip or partially on-chip optics holds advantages in footprint, cost, and timescale while maintaining the same sensitivity as similar techniques (Bates and Lu, 2016).

2.4.1. Optical waveguide sensors

Optical waveguides, which have many outstanding advantages such as sensitivity, simple structure, small physical volume, ease of assembly, resistance to corrosion and good insulation, can be used to fabricate various sensors. Miniaturized optical fibres have been successfully integrated into microfluidic and LOC systems. Simultaneously, now that semiconductor fabrication methods are well established, more miniaturized photonic devices, such as multiplexed optical fibre systems divided according to space, time or wavelength, are replacing simple, discrete optical fibres in the fabrication of more complex fluidic microsystems (Blue and Uttamchandani, 2016). A microspectrometer of monolithic integrated arrayed-waveguide gratings (AWGs) was employed to resolve different visible wavelengths, thereby enabling multiplexed analysis (Hu et al., 2012). A similar integrated lensed AWG microspectrometer was developed by the same group for localized fluorescence measurements (Fig. 5). The intensity levels of several fluorescence signals were measured simultaneously by simple CCD camera readouts. In order to improve signal collection and spatial resolution, the shape of the beam was confined by a lensing function for focused illumination (Hu et al., 2014).

Silicon photonic wire waveguides are one of the most sensitive optical transducers for label-free sensing; their extremely small size and high refractive index confer a strong interaction between the light guided and molecules bound on the waveguide surface (Janz et al., 2013). An array of silicon photonic wire waveguide sensors was integrated into a microfluidic chip. The binding of different molecules could be monitored simultaneously. The real-time antibody-antigen reactions were monitored with an LOD of less than 0.3 pg/mm^2 by using IgG receptor-analyte complementary pairs and unpaired bovine serum albumin (Densmore et al., 2009). The same research group also fabricated another complete photonic-wire molecular biosensor microarray chip (Fig. 6). The sensor chips were interrogated by an

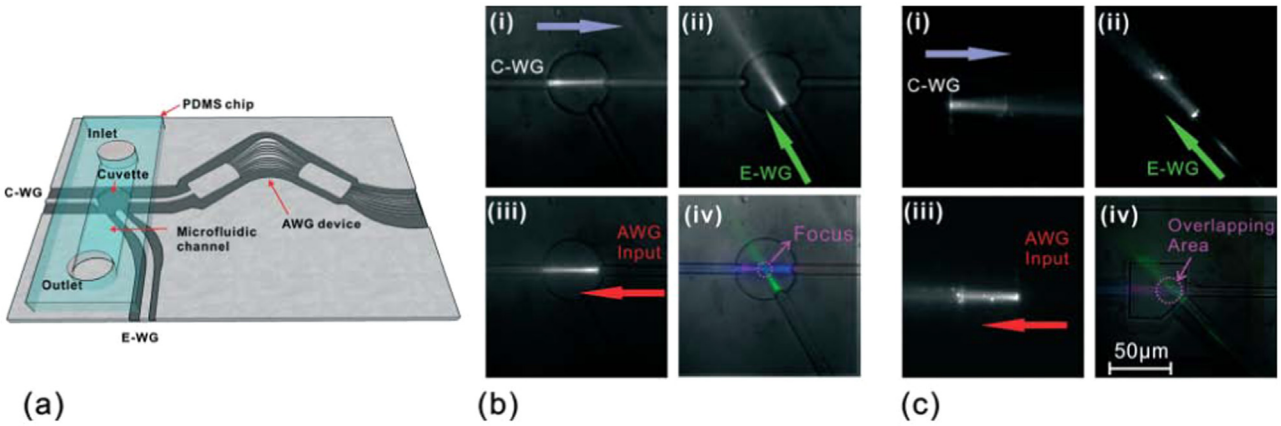

Fig. 5. (a) Schematic of an AWG integrated microfluidic platform. (b) and (c) are fluorescence microscopy images of the system with the lens and flat-end waveguides, respectively (Hu et al., 2014). Reproduced by permission of The Royal Society of Chemistry.

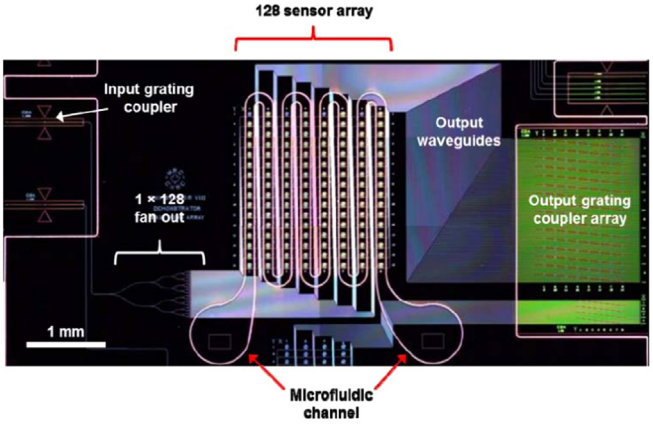

Fig. 6. A microscope image of a sensor chip, showing a different layout. Reprinted (adapted) with permission from Janz et al. (2013). Copyright 2013, the Optical Society.

automatic instrument that could deliver samples and acquire up to 128 optical sensor outputs simultaneously in real time. Serotyping of *E. coli* bacteria was used to demonstrate the multiplexed assay (Janz et al., 2013). A conceptual paradigm based on the interaction between surface and photonic-band-gap waveguides promotes the optical biosensing of multiple diseases through LOC. It was shown by simulations that levels of light transmission through the photonic crystal in the device responded simultaneously to analyte binding and layer thicknesses of corresponding sites. In contrast to single resonance shift in traditional biosensing, this multiparametric biosensing mechanism provides a more thorough data fingerprint useful for discriminating subtle differences in the sample. Logically, the spectral line shape can also be used to discriminate different concentrations of several analytes (Alrashid and John, 2015). The integration of silicon photonic biosensors in a system level was realized using Fan-Out Wafer-Level-Packaging toward low cost and multiplexed point-of-care diagnostic testing (Laplatine et al., 2018).

2.4.2. Whispering-gallery mode optical biosensors

Optical microdevices based on highly sensitive whispering-gallery mode biosensors (WGMBs) have been developed for sensitive and real-time biodetection. This kind of sensors was also integrated with precise microfluidics control to achieve label-free and real-time detection of cell biomarker release in real time and with nanomolar sensitivity (Chen et al., 2018). In the same way as other optics sensors, WGMB with the immobilization of different antibody can be used to realize multiplex detection. With different sensing location, the specific release of biomarkers within a complex organ-on-a-chip can also be realized.

2.4.3. Interferometric silicon chip sensors

One sensor chip consisting an array of 10 broad-band Mach-Zehnder interferometers (BB-MZIs) monolithically integrated on silicon, was combined with microfluidic module for the simultaneous, label-free immunochemical determination of four allergens. The immunoreaction occurred on BB-MZIs were monitored by multiplexing their transmission spectra through an external miniaturized spectrometer (Angelopoulou et al., 2018; Anastasopoulou et al., 2018).

2.4.4. Lens-free diffraction on-chip sensing

Plasmonic nanoapertures illuminated by a quasi-coherent and quasi-monochromatic source were used at the bottom of a microfluidic channel to develop lens-free on-chip sensing. Lens-free diffraction patterns of metallic nanoapertures were recorded by an optoelectronic sensor array. These patterns were further processed to create digital transmission patterns. The analysis of the cross-correlation among these patterns allowed the sensing of the local refractive index in the near field of the plasmonic nanoapertures. This on-chip sensing approach is useful for the development of microfluidic label-free multiplexing sensors (Khademhosseinieh et al., 2010).

2.5. Optical sensors in digital microfluidic systems

Digital microfluidic LOC technology offers a testing platform with high throughput, portability, an increased level of automation and the possibility of mass production. However, there is a limited capacity for most digital microfluidic (DMF) platforms to integrate with sensing because it is difficult to integrate complex optical functions into the DMF platform. The advent of heterogeneous photonic element integration technologies, such as refraction index sensors (SPR sensors, microresonator sensors, etc.) and planar optical systems (thin-film semiconductor devices), brings many opportunities to introduce more complex photonics components for optical functions onto arbitrary host substrates and integrate them into microfluidic systems. For example, a study on the use of an InGaAs thin-film photodetector-based planar optical sensor was the first report on the introduction of optical sensing systems into a digital platform (Lin et al., 2008). An in situ spectroscopic analysis in DMF systems was demonstrated using conventional light sources and spectrometers, together with optical fibre assemblies that directed light towards and collected light from the fluid. Light propagation in the plane of the DMF chip was used to enhance the interaction length. This solution helps overcome the sensitivity limitations of conventional vertical absorbance measurements (Srinivasan et al., 2004; Wijethunga et al., 2011). In addition to absorbance

(Srinivasan et al., 2004; Wijethunga et al., 2011) and electrochemiluminescence (Shamsi et al., 2016) measurements, in situ label-free detection in DMF systems was shown by using functionalized SPR sensors on the top substrate of a DMF system (Malic et al., 2009), but this approach was also limited to the detection of a single analyte per DMF cell. As an alternative, optical microresonators have been integrated into DMF systems (Lerma et al., 2012; Luan et al., 2012; Royal et al., 2013; Wondimu et al., 2017). These devices feature small footprints and lend themselves to integration in the form of large-scale sensor arrays for simultaneous multicomplex detection in a single DMF cell. A multisensor chip comprising an array of whispering-gallery-mode (WGM) microgoblet lasers was integrated into a DMF system. The lasers were fabricated from PMMA doped with dye. Reading the devices via simple free-space optics allowed large-scale sensor arrays to be addressed. The specific binding of streptavidin to a biotinylated sensor surface was then measured by bulk refractive index sensing. That study marked the first use of optical cavities in label-free detection of biomolecules in a DMF system (Geidel et al., 2016).

2.6. Multiplex integration toward labs on chip

Beyond the use of microfluidic chip channel for sample transfer, there are also reports concentrating on the combination of multiple sophisticated biochemical steps and multi-sensors based on different principles into a monolithic, portable and powerful labs on chip device.

2.6.1. The integration of more functional modules

A new microfluidic cartridge with multiple integrated silicon nitride optical ring resonators, incorporated a photonic biosensor and electrochemical pumps, was reported for immunoassays (Geidel et al., 2016). Another multiplexed assay platform for disease-specific DNA sequences was constructed by utilizing a camera from a cell phone as the sensor (Fig. 6). A hand-held “cradle” was used to interrogate a microfluidic chip with the cell phone. The chip was embedded within a credit-card-sized cartridge. In approximately 30 min, with a single 15 μL droplet of test sample, the ability of the system was demonstrated by selective qualitative determination of four specific nucleic acid sequences for equine respiratory pathogens with LODs comparable to those obtained through laboratory-based methods. The target nucleic acid sequences in the sample combined with the reagents for loop-mediated isothermal amplification (LAMP) which were predeposited into different channels of the microfluidic chip. Fluorescent products excited under LEDs could be observed and analysed automatically by the microprocessor in smartphone (Chen et al., 2017) (Fig. 7).

Another marketable LOC characterized by a high degree of integration of modularity for multiparameter analyses was reported. Microfluidic actuators, reagents, and various sensors were integrated into a self-contained cartridge. In combination with automatic data acquisition and a data analysis unit with a user-friendly interface, the detection of nucleic acids and protein markers was realized through a redox-cycling-based electrochemical read-out and a total internal reflectance fluorescence (TIRF)-based optical read-out (Schumacher et al., 2012). There is a review focusing on the translation of microfluidic biosensing technology for point-of-care (POC) diagnostic applications (Kumar et al., 2014).

2.6.2. Multiplex sensors in organ-on-a-chip systems

Organ-on-a-chip systems are microfluidic 3D in vitro human tissue and organ models, which are expected not only to replace the traditional planar cell cultures but also to provide the ability to analyse multiorgan interactions with multiple organoid models. In situ continuous measurement is characterized by the combination of several kinds of sensor technology. A system capable of optically and electrochemically monitoring extracellular and intracellular metabolites simultaneously was reported. A sensor electrode array was transiently simulated for electrochemical monitoring of the metabolic activity of ventricular myocytes. The influence of accumulated metabolic by-products was reflected by optical measurement of single muscle cell contraction. The concomitant changes in intracellular calcium transients and pH were detected using different fluorescent dyes (Cheng et al., 2010). Since it is difficult to integrate conventional sensing devices with microfluidic organ-on-a-chip systems with low-volume bioreactors, a multifunctional LOC system to study the brain system in hypoxia was designed. The concentration of oxygen in the channels was monitored by an oxygen sensor. The oxygenation state of chicken red blood cells (RBCs) was verified simultaneously by absorption spectra. The cells could be studied with a long time of viability (Alrifaiy et al., 2007). A sensing system using LEDs and silicon photodiodes for real-time measurement of dissolved oxygen levels and pH in the cell culture medium was constructed. The sensing module consisted of an optically transparent window for measuring light intensity, and this module could be connected directly to the bioreactor without any special modifications to the design of microfluidic device. A user-friendly electronic interface was included to control the optical transducer and signal acquisition from the photodiodes. The dissolved oxygen levels and pH in the culture medium of human dermal fibroblasts were measured continuously

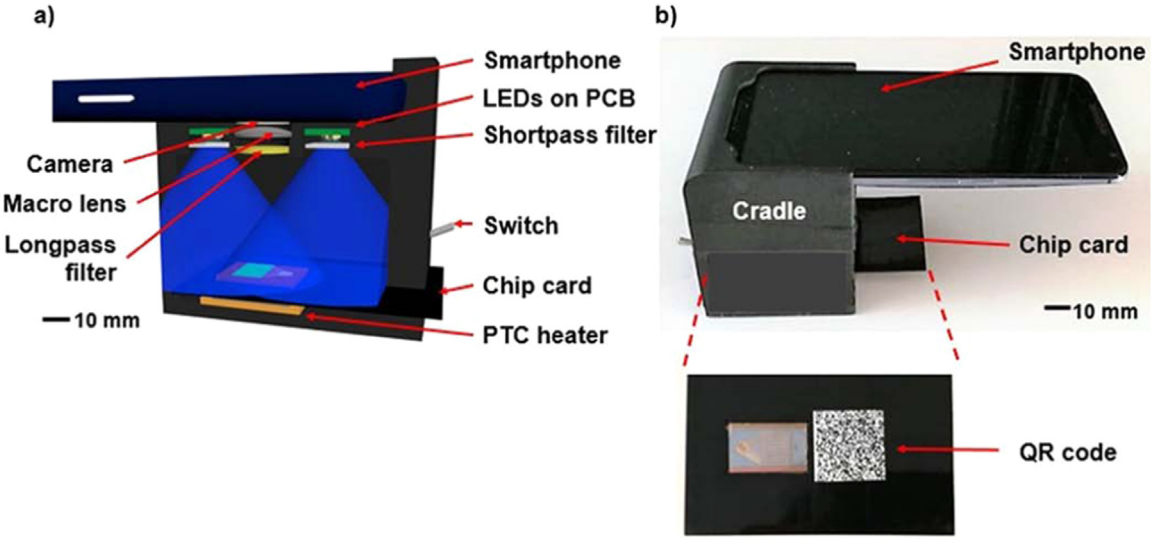

Fig. 7. (a) Schematic of the internal structure of the cradle including optical and electrical components. (b) Photograph of the instrument with the smartphone and chip card. Reprinted (adapted) with permission from Chen et al. (2017). Copyright 2017, American Chemical Society.

for up to 3 days. This microfluidic system provides a new analytical platform that is easy to fabricate and operate and can be adapted for various situations (Mousavi Shaegh et al., 2016). It is believed that an operational organ-on-a-chip model integrating a multitude of physical, biochemistry, and optical sensors will be able to pave the way for automated, high-performance in situ monitoring for drug screening (Zhang et al., 2017).

3. Conclusion

Technological advancements in the fields of microelectromechanical systems (MEMS), materials science, rational design, microfluidics, and sensor printing have radically shaped biosensor technology. New branches of science are originating and overlapping more quickly than ever. The emergence of new physical and chemical effects including nanoplasmonics, new materials such as piezoelectric semiconductor materials and photonic crystals, and many advanced nanotechnologies represented by MEMS and nanomaterials have proven to be of immense help in the continuous effort to develop robust, stable on-chip multiplex optical biosensors that are easy and relatively inexpensive to fabricate and use.

Continuous improvements in order to be more sensitive, high throughput and portable are always the goals of optical sensor technologies. With the unreplaceable merit of integration, miniaturization and portability owned by microfluidic chip, the integration of optical biosensors and microfluidic chip, is also the main trend for multiplex Optical Sensors. Initially, high-density arrays coupled with logic functions on small chip areas have had a profound impact on the fabrication of high-throughput sensors. Gradually, combine biosensors with microfluidic chips have continued to emerge (Ying and Wang, 2013). Sensing platforms integrated with fluidic microsystems can provide further advantages over traditional parallel single-analyte assays, including reduced sample volumes, increased speed and sensitivity, and increased ease of parallel and multisample analysis. Furthermore, there are efforts devoted into the integration of multiplex or hybrid sensors with other functionalities (e.g., cell culture, sample processing, genetic amplification, reaction chambers, and electronic automation) in a compact device to create a portable platform with sample-in-answer-out capability for use in clinical practice, food or environmental analysis, high-throughput screening, POCT and wearable devices (Fair, 2009; Han et al., 2013). Promoted by the foundational work and advances in microelectromechanical system fabrication techniques, significant developments in the integration of various miniaturized solid-state or homogenous optical elements with microfluidic systems have made it possible to perform previously impossible analyses with comparable performance to non-microfluidic systems.

Acknowledgements

This review was supported by the Specially-Funded Programme on National Key Scientific Instruments and Equipment Development (2012YQ04014006), Natural Science Foundation of Shenzhen City (JCYJ20170307150444573).

Conflicts of interest

The authors declare no conflict of interest.

References

Alrashid, A., John, S., 2015. Phys. Rev. Appl. 3 (3).
Alrifaiy, A., Borg, J., Lindahl, O., Ramser, K., 2007. Biomed. Eng. Online 14 (1), 36.
Angelopoulou, M., Petrou, P.S., Makarona, E., Haasnoot, W., Moser, I., Jobst, G., Goustouridis, D., Lees, M., Kalatzi, K., Raptis, I., Misiakos, K., Kakabakos, S.E., 2018. Anal. Chem. 90 (15), 9559–9567.
Anastasopoulou, M., Malainou, A., Salapatas, A., Chronis, N., Raptis, I., Misiakos, K., 2018. Sens. Actuators B Chem. 256, 304–309.
Anker, J.N., Hall, W.P., Lyandres, O., Shah, N.C., Zhao, J., Van Duyne, R.P., 2008. Nat. Mater. 7 (6), 442–453.
Arduini, F., Cinti, S., Scognamiglio, V., Moscone, D., Palleschi, G., 2017. Anal. Chim. Acta 959, 15–42.
Atalay, Y.T., Verboven, P., Vermeir, S., Vergauwe, N., Nicolaï, B., Lammertyn, J., 2009. Microfluid. Nanofluid. 7 (3), 393.
Bakaltcheva, I.B., Ligler, F.S., Patterson, C.H., Shriver-Lake, L.C., 1999. Anal. Chim. Acta 399 (1–2), 13–20.
Basabedesmonts, L., Benitolópez, F., Gardeniers, H.J., Duwel, R., Van, d.B.A., Reinhoudt, D.N., Cregocalama, M., 2008. Anal. Bioanal. Chem. 390 (1), 307–315.
Bates, K.E., Lu, H., 2016. Biophys. J. 110 (8), 1684–1697.
Bigdeli, A., Ghasemi, F., Golmohammadi, H., Abbasi-Moayed, S., Maf, N., Fahimi-Kashani, N., Jafarinejad, S., Shahrajabian, M., Hormozi-Nezhad, M.R., 2017. Nanoscale 9, 43.
Bilge, E., Deniz, Y.M., Stefan, S., Gardeniers, J.G.E., Jurriaan, H., 2011. Int. J. Mol. Sci. 12 (11), 7335–7351.
Biswas, A., Bayer, I.S., Biris, A.S., Wang, T., Dervishi, E., Faupel, F., 2012. Adv. Colloid Interface Sci. 170 (1–2), 2–27.
Blue, R., Uttamchandani, D., 2016. J. Biophoton. 9 (1–2), 13–25.
Bunyakul, N., Baeumner, A.J., 2014. Sensors 15 (1), 547–564.
Burton, R.E., White, E.J., Foss, T.R., Phillips, K.M., Meltzer, R.H., Kojanian, N., Kwok, L.W., Lim, A., Pellerin, N.L., Mamaeva, N.V., 2010. Lab Chip 10 (7), 843–851.
Cao, J., Sun, T., Grattan, K.T.V., 2014. Sens. Actuators B Chem. 195 (5), 332–351.
Cao, L., Cheng, L., Zhang, Z., Wang, Y., Zhang, X., Chen, H., Liu, B., Zhang, S., Kong, J., 2012. Lab Chip 12 (22), 4864–4869.
Carlborg, C.F., Gylfason, K.B., Kaźmierczak, A., Dortu, F., Bañuls Polo, M.J., Maquieira, C.A., Kresbach, G.M., Sohlström, H., Moh, T., Vivien, L., 2010. Lab Chip 10 (3), 281–290.
Cetin, A.E., Coskun, A.F., Galarreta, B.C., Huang, M., Herman, D., Ozcan, A., Altug, H., 2014. Light Sci. Appl. 3 (1), e122.
Chang, T.Y., Huang, M., Yanik, A.A., Tsai, H.Y., Shi, P., Aksu, S., Yanik, M.F., Altug, H., 2011. Lab Chip 11 (21), 3596–3602.
Chen, G., Wang, Y., Wang, H., Cong, M., Chen, L., Yang, Y., Geng, Y., Li, H., Xu, S., Xu, W., 2014. Rsc Adv. 4 (97), 54434–54440.
Chen, P., Meng, T.C., Mchugh, W., Nidetz, R., Li, Y., Fu, J., Cornell, T.T., Shanley, T.P., Kurabayashi, K., 2015. Acs Nano 9 (4), 4173.
Chen, W., Yu, H., Sun, F., Ornob, A., Brisbin, R., Ganguli, A., Vemuri, V.K., Strzebonski, P., Cui, G., Allen, K.J., 2017.
Chen, Y., Nakamoto, K., Niwa, O., Corn, R.M., 2012. Langmuir 28 (22), 8281–8285.
Chen, Y.J., Schoeler, U., Huang, C.H., Vollmer, F., 2018. Small 14, 22a.
Cheng, I., Chang, H.C., Chen, T.Y., Hu, C., Yang, F.L., 2013. vol. 3 (3), 2365.
Cheng, W., Klauke, N., Smith, G., Cooper, J.M., 2010. Electrophoresis 31 (8), 1405–1413.
Choi, N., Lee, K., Lim, D.W., Lee, E.K., Chang, S.I., Oh, K.W., Choo, J., 2012. Lab Chip 12 (24), 5160–5167.
Chou, J., Wong, J., Christodoulides, N., Floriano, P.N., Sanchez, X., Mcdevitt, J., 2012. Sensors 12 (11), 15467.
Cooper, M.A., 2006. Drug Discov. Today 11 (23), 1061–1067.
Coskun, A.F., Cetin, A.E., Galarreta, B.C., Alvarez, D.A., Altug, H., Ozcan, A., 2014. Sci. Rep. 4 (4) (6789-6789).
Cuiffi, J., Soong, R., Manolakos, S., Mohapatra, S., Larson, D., 2010. Ifmbe Proc. 32, 572–575.
Densmore, A., Vachon, M., Xu, D.X., Janz, S., Ma, R., Li, Y.H., Lopinski, G., Delâge, A., Lapointe, J., Luebbert, C.C., 2009. Opt. Lett. 34 (23), 3598–3600.
Douglass, P.M., Salins, L.L., Dikici, E., Daunert, S., 2002. Bioconjugate Chem. 13 (6), 1186–1192.
Ebbesen, T.W., Lezec, H.J., Ghaemi, H.F., Thio, T., Wolff, P.A., 1998. Nature 391 (6), 1114–1117.
Ehgartner, J., Strobl, M., Bolivar, J.M., Rabl, D., Rothbauer, M., Ertl, P., Borisov, S.M., Mayr, T., 2016. Anal. Chem. 88 (19), 9796–9804.
Emmerson, G.D., Gawith, C.B.E., Smith, P.G.R., 2010. Multiwavelength optical sensors. US.
Escobedo, C., 2013. Lab Chip 13 (13), 2445–2463.
Estevez, M.C., Otte, M.A., Sepulveda, B., Lechuga, L.M., 2014. Anal. Chim. Acta 806 (806C), 55–73.
Fair, R.B., 2009. Conf. Proc. IEEE Eng. Med. Biol. Soc. 2009 (2009), 6560–6564.
Fan, X., White, I.M., Shopova, S.I., Zhu, H., Suter, J.D., Sun, Y., 2008. Anal. Chim. Acta 620 (1), 8–26.
Faulds, K., Mckenzie, F., Smith, W.E., Graham, D., 2010. Angew. Chem. 119 (11), 1861–1863.
Ferguson, J.A., Boles, T.C., Adams, C.P., Walt, D.R., 1996. Nat. Biotechnol. 14 (13), 1681–1684.
Ferrier, D.C., Shaver, M.P., Hands, P.J., 2015. Biosens. Bioelectron. 68, 798–810.
Ge, X., Asiri, A.M., Du, D., Wen, W., Wang, S., Lin, Y., 2014. Trends Anal. Chem. 58, 31–39.
Geidel, S., Llopis, S.P., Rodrigo, M., Diego-Castilla, G.D., Sousa, A., Nestler, J., Otto, T., Gessner, T., Parro, V., 2016. Micromachines 7 (9), 153.
Ghasemi, F., Hosseini, E.S., Song, X., Gottfried, D.S., Chamanzar, M., Raeiszadeh, M., Cummings, R.D., Eftekhar, A.A., Adibi, A., 2016. Biosens. Bioelectron. 80, 682–690.
Grimaldi, I.A., Testa, G., Bernini, R., 2015. Rsc Adv. 5 (86), 70156–70162.
Guan, C., Liu, Z., Yang, J., 2010. Plasma resonant type optical fiber biosensor based on annular core wave guide.
Han, K.N., Li, C.A., Seong, G.H., 2013. Annu. Rev. Anal. Chem. 6 (1), 119–141.
Herzog, C., Beckert, E., Nagl, S., 2014. Anal. Chem. 86 (19), 9533–9539.
Herzog, C., Poehler, E., Peretzki, A.J., Borisov, S.M., Aigner, D., Mayr, T., Nagl, S., 2016. Lab Chip 16 (9), 1565–1572.
Heyduk, E., Dummit, B., Chang, Y.H., Heyduk, T., 2008. Anal. Chem. 80 (13), 5152–5159.

Holzinger, M., Goff, A.L., Cosnier, S., 2014. Front. Chem. 2 (4), 63.
Hu, Z., Glidle, A., Ironside, C., Cooper, J.M., Yin, H., 2014. Lab Chip 15 (1), 283–289.
Hu, Z., Glidle, A., Ironside, C., Sorel, M., Strain, M., Cooper, J., Yin, H., 2012. Lab Chip 12 (16), 2850–2857.
Huang, J.A., Zhang, Y.L., Ding, H., Sun, H.B., 2015. Adv. Opt. Mater. 3 (5), 618–633.
Ince, R., Narayanaswamy, R., 2006. Anal. Chim. Acta 569 (1), 1–20.
Jackman, J.A., Rahim, F.A., Cho, N.J., 2017. Chem. Soc. Rev. 46 (12), 3615.
Jadon, N., Jain, R., Sharma, S., Singh, K., 2016. Talanta 161, 894–916.
Jang, E., Kim, S., Koh, W.G., 2012. Biosens. Bioelectron. 31 (1), 529–536.
Janz, S., Xu, D.X., Vachon, M., Sabourin, N., Cheben, P., Mcintosh, H., Ding, H., Wang, S., Schmid, J.H., Delâge, A., 2013. Opt. Express 21 (4), 4623–4637.
Jiang, Y., Wang, H., Li, S., Wen, W., 2014. Sensors 14 (4), 6952.
Jokerst, J.V., Raamanathan, A., Christodoulides, N., Floriano, P.N., Pollard, A.A., Simmons, G.W., Wong, J., Gage, C., Furmaga, W.B., Redding, S.W., 2009. Biosens. Bioelectron. 24 (12), 3622–3629.
Kelley, S.O., Mirkin, C.A., Walt, D.R., Ismagilov, R.F., Toner, M., Sargent, E.H., 2014. Nat. Nanotechnol. 9 (12), 969–980.
Khademhosseinieh, B., Biener, G., Sencan, I., Su, T.W., Coskun, A.F., Ozcan, A., 2010. Appl. Phys. Lett. 97 (22), 39.
Kneipp, K., Kneipp, H., Itzkan, I., Dasari, R.R., Feld, M.S., 2002. J. Phys. Condens. Matter 14 (18), R597.
Kumar, S., Kumar, S., Ali, M.A., Anand, P., Agrawal, V.V., John, R., Maji, S., Malhotra, B.D., 2014. Biotechnol. J. 8 (11), 1267–1279.
Kwon, M.S., Steier, W.H., 2008. Opt. Express 16 (13), 9372–9377.
Lafleur, J.P., Jönsson, A., Senkbeil, S., Kutter, J.P., 2016. Biosens. Bioelectron. 76, 213–233.
Laplatine, L., Luan, E.X., Cheung, K., Ratner, D.M., Dattner, Y., Chrostowski, L., 2018. Sens. Actuators B-Chem. 273, 1610–1617.
Le, N.T., Kim, J.S., 2014. J. Nanosci. Nanotechnol. 14 (12), 9465–9469.
Lerma, A.C., Witters, D., Puers, R., Lammertyn, J., Bienstman, P., 2012. Anal. Bioanal. Chem. 404 (10), 2887–2894.
Lertvachirapaiboon, C., Baba, A., Ekgasit, S., Shinbo, K., Kato, K., Kaneko, F., 2017. Jpn. J. Appl. Phys. 56 (1).
Li, X., Soler, M., CI, Ö., Belushkin, A., Yesilköy, F., Altug, H., 2017. Lab Chip 17 (13).
Lin, F., Zhao, X., Wang, J., Yu, S., Deng, Y., Geng, L., Li, H., 2014. Analyst 139 (11), 2890–2895.
Lin, L., Evans, R.D., Nan, M.J., Fair, R.B., 2008. IEEE Sens. J. 8 (5), 628–635.
Liu, C., Cui, D., Li, H., 2011. Biosens. Bioelectron. 26 (1), 255–261.
Liu, Z.H., Yang, X.H., Zhang, Y., Zhang, Y.X., Zhu, Z.D., Yang, X.H., Zhang, J.Z., Yang, J., Yuan, L.B., 2018. Sens. Actuators B Chem. 265, 211–216.
Liu, X.H., Li, H., Zhao, Y.J., Yu, X.D., Xu, D.K., 2018. Talanta 188, 417–422.
Long, Y.T., Jing, C., 2014. Springerbriefs in Molecular Science.
Lu, Y., Yu, S., Lin, F., Lin, F., Zhao, X., Wu, L., Miao, Y., Li, H., Deng, Y., Geng, L., 2017. Analyst 142 (22), 4257.
Luan, C., Xu, Y., Chen, B., Yang, Z., 2017. Sens. Actuators B Chem. 242, 1259–1264.
Luan, L., Royal, M.W., Evans, R., Fair, R.B., Nan, M.J., 2012. IEEE Sens. J. 12 (6), 1794–1800.
Malic, L., Veres, T., Tabrizian, M., 2009. Biosens. Bioelectron. 24 (7), 2218–2224.
Mayer, K.M., Hafner, J.H., 2011. Chem. Rev. 111 (6), 3828–3857.
Mousavi Shaegh, S.A., De, F.F., Zhang, Y.S., Nabavinia, M., Binth, M.N., Ryan, J., Pourmand, A., Laukaitis, E., Banan, S.R., Nadhman, A., 2016. Biomicrofluidics 10 (4), 760–793.
Muzyka, K., 2014. Biosens. Bioelectron. 54 (15), 393–407.
Nguyen, H.H., Park, J., Kang, S., Kim, M., 2015. Sensors 15 (5), 10481–10510.
Nyholm, L., 2005. Analyst 130 (5), 599–605.
Qi, J., Li, B., Wang, X., Zhang, Z., Wang, Z., Han, J., Chen, L., 2017. Sens. Actuators B Chem. 251.
Rampazzi, S., Danese, G., Leporati, F., Marabelli, F., 2016. IEEE Trans. Instrum. Meas. 65 (2), 317–327.
Rocha-Santos, T.A.P., 2014. Trends Anal. Chem. 62, 28–36.
Royal, M.W., Nan, M.J., Fair, R.B., 2013. IEEE Sens. J. 13 (12), 4733–4742.
Sabhachandani, P., Cohen, N., Sarkar, S., Konry, T., 2015. Microchim. Acta 182 (9–10), 1835–1840.
Sang, S., Zhao, Y., Zhang, W., Li, P., Hu, J., Li, G., 2014. Biosens. Bioelectron. 51 (3), 124–135.
Schumacher, S., Nestler, J., Otto, T., Wegener, M., Ehrentreich-Förster, E., Michel, D., Wunderlich, K., Palzer, S., Sohn, K., Weber, A., 2012. Lab Chip 12 (3), 464–473.
Shamsi, M.H., Choi, K., Ng, A.H., Dean, C.M., Wheeler, A.R., 2016. Biosens. Bioelectron. 77, 845–852.
Shen, S., Jia, M., Tang, Z., 2018. Mater. Res. Bull. 106, 471–477.
Singh, P., 2016. Sens. Actuators B Chem. 229 (3), 110–130.
Špačková, B., Wrobel, P., Bocková, M., Homola, J., 2016. Proc. IEEE 104 (12), 2380–2408.
Srinivasan, V., Pamula, V., Pollack, M., Fair, R., 2003. In: A Digital Microfluidic Biosensor for Multianalyte Detection. IEEE the Sixteenth International Conference on MICRO Electro Mechanical Systems. Mems-03 Kyoto, pp. 327–330.
Srinivasan, V., Pamula, V.K., Fair, R.B., 2004. Lab Chip 4 (4), 310–315.
Steiner, G., 2004. Anal. Bioanal. Chem. 379 (3), 328–331.
Surade, S., Klein, M., Stolt-Bergner, P.C., Muenke, C., Roy, A., Michel, H., 2010. Chem. Soc. Rev. 39 (11), 4234–4243.
Ueno, Y., Furukawa, K., Matsuo, K., Inoue, S., Hayashi, K., Hibino, H., 2015. Anal. Chim. Acta 866, 1–9.
Van, R.A., de Jong, A.M., den Toonder, J.M., Prins, M.W., 2014. Lab Chip 14 (12), 1966–1986.
Wang, H.Q., Wu, Z., Tang, L.J., Yu, R.Q., Jiang, J.H., 2011. Nucleic Acids Res. 39 (18), e122.
Wang, L., Yan, R., Huo, Z., Wang, L., Zeng, J., Bao, J., Wang, X., Peng, Q., Li, Y., 2010. Angew. Chem. 117 (37), 6208–6211.
Wijethunga, P.A.L., Nanayakkara, Y.S., Kunchala, P., Armstrong, D.W., Moon, H., 2011. Anal. Chem. 83 (5), 1658–1664.
Wondimu, S.F., Von, d.E.S., Ahrens, R., Freude, W., Guber, A.E., Koos, C., 2017. Lab Chip 17 (10), 1740–1748.
Yavas, O., Acimovic, S.S., Garcia-Guirado, J., Berthelot, J., Dobosz, P., Sanz, V., Quidant, R., 2018. ACS Sensors 3 (7), 1376–1384.
Ying, L., Wang, Q., 2013. BMC Biotechnol. 13 (1).
Zhang, Y.S., Aleman, J., Shin, S.R., Kilic, T., Kim, D., Mousavi Shaegh, S.A., Massa, S., Riahi, R., Chae, S., Hu, N., 2017. Proc. Natl. Acad. Sci. USA 114 (12), E2293.
Zhou, Q., Kim, T., 2016. Sens. Actuators B Chem. 227, 504–514.